

- [1] Y. C. Lee, R. T. Lee in *Neoglycoconjugates: Preparation and Applications*, Academic Press, San Diego, **1994**.
- [2] a) N. V. Bovin, H. J. Gabius, *Chem. Soc. Rev.* **1995**, 24, 413–422; b) R. Roy, *Curr. Opin. Struct. Biol.* **1996**, 6, 692–702; c) P. D. Rye, *Biotechnology* **1997**, 14, 155–157.
- [3] a) R. Roy, W. K. C. Park, O. P. Srivastava, C. Foxall, *Bioorg. Med. Chem. Lett.* **1996**, 6, 1399–1402; b) H. Miyauchi, M. Tanaka, H. Koike, N. Kawamura, M. Hayashi, *Bioorg. Med. Chem. Lett.* **1997**, 7, 985–988; c) E. J. Gordon, W. J. Sanders, L. L. Kiessling, *Nature* **1998**, 392, 30–31; d) G. Thoma, J. T. Patton, J. L. Magnani, B. Ernst, R. Öhrlein, R. O. Duthaler, *J. Am. Chem. Soc.* **1999**, 121, 5919–5929.
- [4] a) H. Dohi, Y. Nishida, M. Mizuno, M. Shinkai, T. Kobayashi, T. Takeda, H. Uzawa, K. Kobayashi, *Bioorg. Med. Chem.* **1999**, 7, 2053–2062; b) P. I. Kitov, J. M. Sadowska, G. Mulvey, G. D. Armstrong, H. Ling, N. S. Pannu, R. J. Read, D. R. Bundle, *Nature* **2000**, 403, 669–672.
- [5] For a recent paper, see H. Dohi, Y. Nishida, Y. Furuta, H. Uzawa, S.-I. Yokoyama, S. Ito, H. Mori, K. Kobayashi, *Org. Lett.* **2002**, 4, 355–357.
- [6] Y. Nishida, H. Uzawa, T. Toba, K. Sasaki, H. Kondo, K. Kobayashi, *Biomacromolecules* **2000**, 1, 68–74.
- [7] C. Mistuoka, M. Sawada-Kasugai, K. Ando-Furui, M. Izawa, H. Nakanishi, S. Nakamura, H. Ishia, M. Kiso, R. Kannagi, *J. Biol. Chem.* **1998**, 273, 11225–11233.
- [8] H. Uzawa, T. Toba, Y. Nishida, K. Kobayashi, N. Minoura, K. Hiratani, *Chem. Commun.* **1998**, 2311–2312, and references therein.
- [9] For the synthetic procedure for the preparation of these glycopolymers, see ref. [6]. Selected data for copolymer **6**, **7**, **8**, and terpolymer **9** are as follows: **6**:  $M_n = 3.1 \times 10^5$ ,  $M_w/M_n = 1.86$  (size-exclusion chromatography (SEC) in phosphate buffer saline (pH 7.4), calibrated with pullulans);  $^1\text{H}$  NMR (500 MHz,  $\text{D}_2\text{O}$ , 60 °C):  $\delta = 7.36$  (brs, 2H, aromatic-H), 7.06 (brs, 2H, aromatic-H), 4.91 (brs, 1H; Fuc H-1), 4.61 (brd, 1H,  $J = 8.5$  Hz; Gal H-1), 4.40–3.53 (brm, 15H), 2.40–2.17 (brm,  $\text{CHCH}_2$ ), 1.79–1.45 (brm,  $\text{CHCH}_2$ ), 1.11 ppm (brs, 1H; Fuc H-6); ( $\text{Le}^x$ :acrylamide = 11:89). **7**:  $M_n = 3.0 \times 10^5$ ,  $M_w/M_n = 1.87$  (SEC in phosphate buffer saline (pH 7.4), calibrated with pullulans);  $^1\text{H}$  NMR (500 MHz,  $\text{D}_2\text{O}$ , 60 °C):  $\delta = 7.56$  (brs, 2H, aromatic-H), 7.25 (brs, 2H, aromatic-H), 5.11 (brs, 1H, Fuc H-1), 4.91 (brd, 1H,  $J = 7.0$  Hz, Gal H-1), 4.50–3.84 (brm, 15H), 2.60–2.30 (brm,  $\text{CHCH}_2$ ), 2.00–1.75 (brm,  $\text{CHCH}_2$ ), 1.32 ppm (brd, 1H,  $J = 6.5$  Hz, Fuc H-6); ( $3'$ -sulfo- $\text{Le}^x$ :acrylamide = 8:92). **8**:  $M_n = 3.1 \times 10^5$ ,  $M_w/M_n = 1.74$  (SEC in phosphate buffer saline (pH 7.4), calibrated with pullulans);  $^1\text{H}$  NMR (500 MHz,  $\text{D}_2\text{O}$ , 60 °C):  $\delta = 7.60$  (brs, 2H, aromatic-H), 7.27 (brs, 2H, aromatic-H), 5.32 (brs, 1H, GlcNAc H-1), 4.57 (brs, 1H), 4.42 (brs, 1H), 4.19 (brs, 1H), 4.00 (brs, 1H), 3.85 (brm, 1H), 3.78 (brm, 1H), 2.52–2.22 (brm,  $\text{CHCH}_2$ ), 2.10 (brs, 3H,  $\text{COCH}_3$ ), 2.00–1.75 (brm,  $\text{CHCH}_2$ ); (6-sulfo-GlcNAc:acrylamide = 10:90). **9**:  $M_n = 2.4 \times 10^5$ ,  $M_w/M_n = 1.77$  (SEC analysis in phosphate buffer saline (pH 7.4), calibrated with pullulans);  $^1\text{H}$  NMR (500 MHz,  $\text{D}_2\text{O}$ , 60 °C):  $\delta = 7.58$  (brm, 4H, aromatic-H), 7.23 (brm, 4H, aromatic-H), 5.32 (brs, 1H, GlcNAc H-1), 5.11 (brs, 1H, Fuc H-1), 4.90 (brs, 1H, Gal H-1), 4.60–3.78 (brm, 22H), 2.60–2.30 (brm,  $\text{CHCH}_2$ ), 2.20 (brs, 3H  $\text{COCH}_3$ ), 2.12–1.75 (brm,  $\text{CH-CH}_2$ ), 1.29 ppm (brs, 1H, Fuc H-6); ( $3'$ -sulfo- $\text{Le}^x$ : 6-sulfo-GlcNAc:acrylamide = 7:6:87).
- [10] H. Ohmoto, K. Nakamura, T. Inoue, N. Kondo, Y. Inoue, K. Yoshino, H. Kondo, *J. Med. Chem.* **1996**, 39, 1339–1343.
- [11] For a recent review, see E. E. Simanek, G. J. McGarvey, J. A. Jablonowski, C.-H. Wong, *Chem. Rev.* **1998**, 98, 833–862.
- [12] L. M. Stoolman, S. D. Rosen, *J. Cell. Biol.* **1983**, 96, 722–729.
- [13] G. Kretzschmar, A. Toepfer, C. Hüls, M. Kause, *Tetrahedron* **1997**, 53, 2485–2494.
- [14] a) K. G. Bowman, B. N. Cook, C. L. Graffenried, C. R. Bertozzi, *Biochemistry* **2001**, 40, 5382–5391; b) R. E. Bruehl, C. R. Bertozzi, S. D. Rosen, *J. Biol. Chem.* **2000**, 275, 32642–32648; c) B. N. Cook, S. Bhakta, T. Biegel, K. G. Bowman, J. I. Armstrong, S. Hemmerich, C. R. Bertozzi, *J. Am. Chem. Soc.* **2000**, 122, 8612–8622.
- [15] A. Patel, T. K. Lindhorst, *J. Org. Chem.* **2001**, 66, 2674–2680.
- [16] P.-H. Amvam-Zollo, P. Sinaï, *Carbohydr. Res.* **1986**, 150, 199–212.

## Attachment of Molecules at a Molecular Printboard by Multiple Host–Guest Interactions\*\*

Jurriaan Huskens,\* Menno A. Deij, and David N. Reinhoudt\*

*Dedicated to Professor Manfred T. Reetz on the occasion of his 60th birthday*

The exact positioning of molecules on surfaces has become essential for the development of molecular electronics<sup>[1]</sup> and biochip applications,<sup>[2]</sup> as well as for conducting single molecule experiments. Commonly, one of two possible routes is followed, either by chemically reacting molecules to surfaces or to anchoring molecules present at a surface, or by physisorption, that is, the use of nonspecific physical interactions between molecule and surface, and between molecules themselves. Covalent chemical modification usually requires synthetic effort, is hard to control at surfaces, and does not allow either self-correction or (intentional) desorption. Physisorption does allow self-correction, which is common for all self-assembly processes, but the thermodynamic and kinetic parameters governing adsorption and desorption are difficult to control. Moreover, neighboring molecule–molecule interactions are usually needed for obtaining stable and ordered layers, thus the formation of densely packed layers is a prerequisite.<sup>[3]</sup>

Supramolecular interactions serve as an intermediate case with the possibility of employing advantages from both routes. Supramolecular interactions, such as those observed in host–guest complexes, are specific and directional, and a wealth of information is usually available on their binding strengths and kinetics. The application of molecules that allow the formation of multiple supramolecular interactions provides a tool to tune adsorption and desorption process parameters because thermodynamics and kinetics are, in principle, straightforwardly related to the number of interactions, and the strength and kinetics of an individual interaction.

It is therefore our goal to apply host surfaces as “molecular printboards” at which multivalent guest molecules can be positioned. Prerequisites will need to be identified to reach thermodynamically and/or kinetically stable assemblies that can be employed in nanotechnology. It is envisaged that one can control adsorption and desorption by environmental stimuli, for example, by competition with another host in solution. Herein we address the thermodynamic and kinetic

[\*] Dr. ir. J. Huskens, Prof. dr. ir. D. N. Reinhoudt, Ir. M. A. Deij  
University of Twente, MESA+ Research Institute  
Laboratory of Supramolecular Chemistry and Technology  
P.O. Box 217, 7500 AE Enschede (The Netherlands)  
Fax: (+31) 53-489-4645  
E-mail: smct@ct.utwente.nl

[\*\*] Dr. Maurice Baars and Prof. Dr. Bert Meijer (TUE) are gratefully acknowledged for supplying the adamantyl-terminated dendrimers. Frank Geurts (Akzo Nobel, Arnhem) is acknowledged for performing the XPS measurements, and Paul Koster for assistance with the grazing-angle FTIR measurements. Szczepan Zapotoczny is acknowledged for performing the AFM measurements. The Dutch Technology Foundation STW is gratefully acknowledged for funding the Simon Stevin Award project on Nanolithography.

issues relating to the use of multiple interactions for stable surface attachment. In the future, this will be extended to real positioning, for example, by the use of dip-pen nanolithography<sup>[4]</sup> for the delivery of molecules to a molecular print-board.

Here, we describe the interaction between adamantyl-(Ad-) functionalized poly(propylene imine) (PPI) dendrimers<sup>[5]</sup> ranging from 4–64 Ad groups per molecule, and self-assembled monolayers (SAMs) of  $\beta$ -cyclodextrin (CD) adsorbates<sup>[6,7]</sup> (a host suitable for the complexation of Ad derivatives<sup>[8]</sup> and capable of forming well-ordered, densely packed monolayers) on gold substrates. The delivery of such dendrimers from solution-phase CD complexes to CD SAMs is described, which makes use of the competition between the solution and the surface host sites, as well as the cooperativity of the surface sites. Furthermore, we will show the possibility of switching between states of slow and fast desorption kinetics by changing the CD concentration in solution, and describe the use of densely packed dendrimer layers and individually imaged and addressed dendrimer molecules.

We prepared SAMs of a  $\beta$ -cyclodextrin heptathioether adsorbate (Figure 1) on gold substrates, as described previously.<sup>[6,8]</sup> We have shown that such adsorbates form densely packed, well-ordered SAMs, the hexagonal packing of which can be visualized by using atomic force microscopy (AFM).<sup>[6]</sup> The binding of small univalent guest molecules to these SAMs has been studied by electrochemical impedance spectroscopy (EIS)<sup>[7]</sup> and surface plasmon resonance (SPR) spectroscopy.<sup>[8]</sup>

The Ad-functionalized PPI dendrimers employed in the present study (generations G2–G4, with 8–32 adamantyl

endgroups, Figure 1) were solubilized in water using an excess of CD in water at pH 2, which ensures the full complexation of all adamantyl groups by CD and protonation of the core amines.<sup>[5a]</sup> Such dendrimer assemblies have been employed as nanocontainers for dye molecules<sup>[5a]</sup> and as nanoreactors for the formation of gold nanoparticles.<sup>[5b]</sup>

By comparison of the molecular sizes of these dendrimers (G2–G4) with the lattice constant (1.7 nm) of the hexagonally ordered CD SAMs, it can be shown that G2 (with 8 Ad endgroups) can interact with only two CD sites simultaneously at a SAM. Analogously, G3 (16 Ad groups) may interact with three CD sites, whereas G4 (32 Ad groups) can access at least four sites. Furthermore, the concentration of the Ad endgroups of G4 matches the CD SAM lattice constant, which makes this dendrimer an especially interesting case for studying cooperativity of surface host sites in binding multivalent guests.

The (intrinsic) binding constant  $K_i$  of an individual Ad–CD interaction is known to be about  $6 \times 10^4 \text{ M}^{-1}$  (25 °C), both in solution and at CD SAMs, as determined previously<sup>[8]</sup> for an Ad guest which closely resembles the Ad endgroups of the dendrimers employed here. The kinetics of such CD complexes commonly follow diffusion-controlled association ( $k_f$  is approximately  $10^9 \text{ M}^{-1} \text{ s}^{-1}$ ), and thus dissociation rates follow directly from this association rate and from thermodynamics.

A mathematical model has been developed in which all Ad–CD interactions are judged to be equal and independent, both in solution and at a SAM, in which cooperativity on the surface is only viewed as an increase of the effective molarity of the CD host upon binding of the first guest site of a

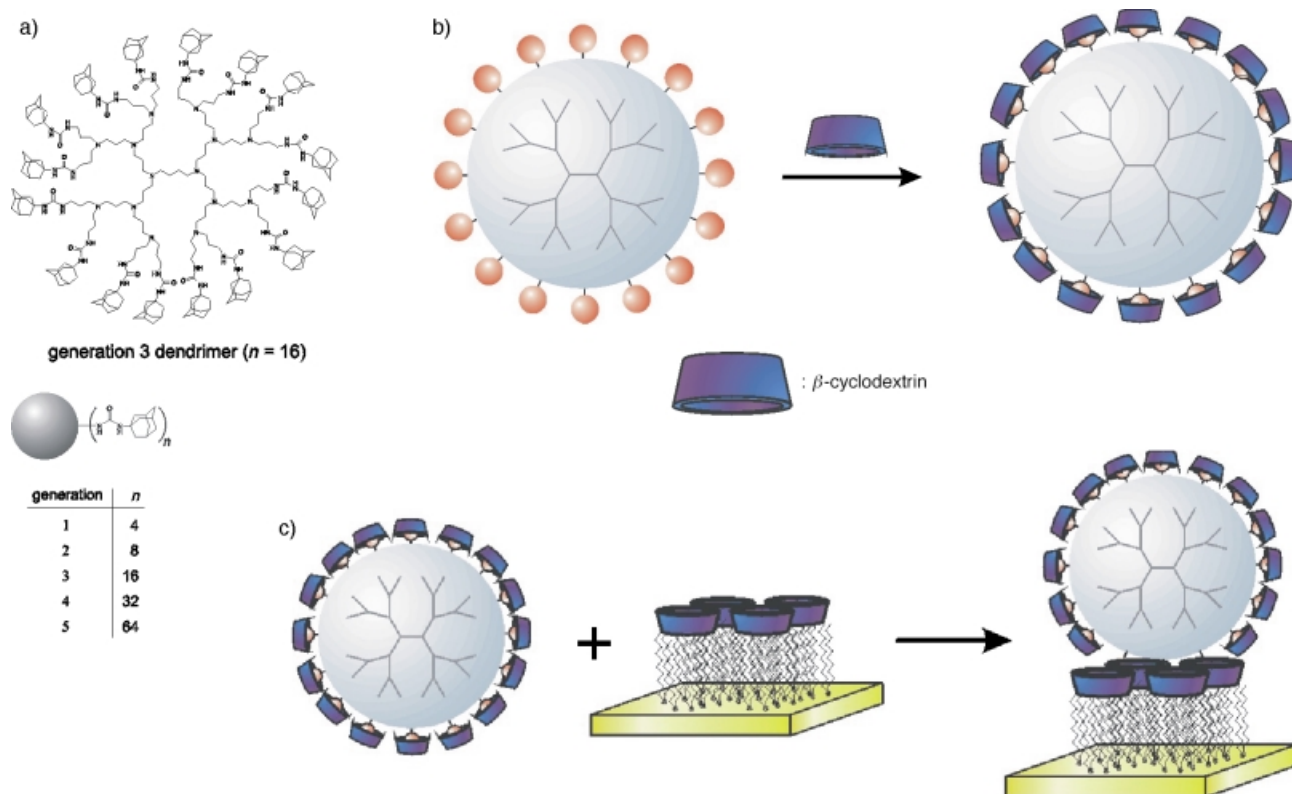


Figure 1. Adamantyl-functionalized poly(propylene imine) dendrimers (a), their formation of water-soluble assemblies by CD (b; see ref. [5a]), and the adsorption of these assemblies onto a CD SAM on gold (c).

multivalent guest.<sup>[9]</sup> This model implies that: a) simultaneous use of at least four CD sites is needed to obtain kinetically slow assemblies under certain conditions, and b) the desorption rate is (positively, but not linearly) dependent on the CD concentration in solution. The results given below are discussed partly as a validation of these model implications.

A CD SAM was immersed in a solution of the G4 dendrimer-CD assemblies, and the adsorption (Figure 1) was studied by SPR spectroscopy. Figure 2a shows a typical SPR time trace in which the adsorption rate and level were studied as a function of dendrimer concentration and of

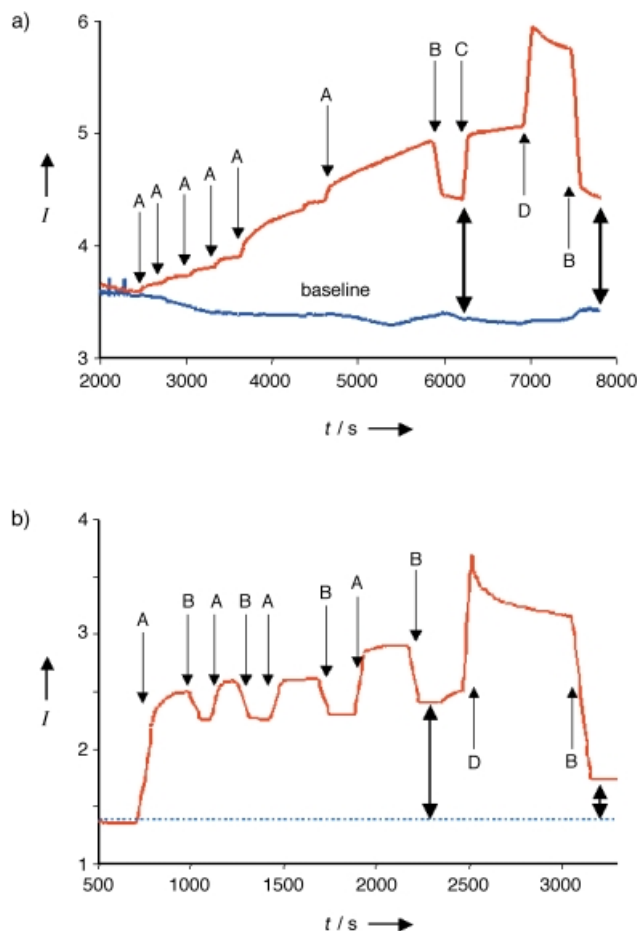


Figure 2. Surface plasmon resonance (SPR) spectroscopy time traces of the adsorption and (attempted) desorption of G4 a) and G3 b) dendrimer-cyclodextrin assemblies onto a CD SAM on a gold substrate; solutions (all in 0.01M aqueous HCl): A) dendrimer-CD, B) 0.01M HCl, C) 1 mM CD, D) 8 mM CD.

washing conditions with 0.01M HCl and 8 mM aqueous CD in 0.01M HCl. These results clearly show the adsorption of dendrimer assemblies at the SAM. Water did not remove the assemblies from the surface, and even 8 mM CD did not lead to detectable desorption under the SPR conditions.

The presence of the dendrimer assemblies after adsorption was verified by FTIR<sup>[10]</sup> and X-ray photoelectron spectroscopy (XPS).<sup>[11]</sup> Water contact angle goniometry shows increased wetting upon adsorption,<sup>[12]</sup> which implies that CD

molecules remain to cover the hydrophobic Ad endgroups of the adsorbed dendrimers at the outer surface. EIS showed an increase of the charge-transfer resistance upon adsorption of G4-CD<sub>32</sub> from 45 to 500 kΩ when the positively charged redox couple [Ru<sup>II</sup>(NH<sub>3</sub>)<sub>6</sub>]<sup>2+</sup>/[Ru<sup>III</sup>(NH<sub>3</sub>)<sub>6</sub>]<sup>3+</sup> was used. This increase results from charge repulsion with the protonated, and thus positively charged, inner core of the dendrimers.<sup>[13]</sup> In principle, the thermodynamics and/or kinetics of adsorption can be studied by using EIS,<sup>[6]</sup> but this was not attempted for practical reasons (relatively slow adsorption, response dependent on charge and thus on protonation degree).

Immersion of a hydroxyundecanethiol SAM in a solution of the G4 assemblies led to nonspecific physisorption as shown by SPR. These assemblies were washed away rapidly, however, using 8 mM CD. As indicated before, the CD SAMs are much less prone to nonspecific adsorption. Combined with the stability of the surface assemblies to water and 8 mM CD, and the different adsorption behavior of individual dendrimers at hydroxy- or CD SAMs (see below), we conclude that the adsorption of the G4 dendrimers at the CD SAMs stems from specific host-guest interactions. As a result of the equal interaction strength of individual Ad-CD interactions in solution and at SAMs, the adsorption solely stems from cooperativity between the surface host sites.

The SPR traces (Figure 2a) do not allow any conclusions regarding the adsorption<sup>[14]</sup> or desorption kinetics. No appreciable desorption occurs in either pure water, or in a relatively concentrated (8 mM) CD solution. In principle, this could be because of thermodynamic stability in the SPR setup and/or the kinetic stability of the surface assemblies. The mathematical model sketched above is indicative of thermodynamic stability in 8 mM CD, rather than kinetic stability, because of the relatively small volume of the CD solution in the SPR setup. In pure water, both thermodynamic and kinetic stability may play a role.

The influence of the number of host-guest interactions on the thermodynamic and kinetic stabilities of the surface assemblies was assessed in the SPR experiments of the G2 and G3 dendrimers. Both showed adsorption from solution (data for G3 shown in Figure 2b). Changing the solution to pure water did not result in loss of material, which indicates thermodynamic and/or kinetic stability of the assemblies. Application of 8 mM CD, however, led to rapid and considerable desorption. The residual signal (20%) in Figure 2b probably reflects a thermodynamic equilibrium in the SPR setup at this CD concentration, which is indicated from both the mathematical model and the relatively high desorption rate.

AFM was used to image and study individual G4 dendrimer assemblies at SAMs. Figure 3a shows an AFM image of a CD SAM immersed for a short time in a dilute solution of G4 assemblies in water. The fact that such assemblies can be imaged at all proves their relative robustness at the CD SAM surface. In contrast, Figure 3c shows islands of G4 dendrimers physisorbed onto a hydroxyundecanethiol SAM. No individual dendrimers can be visualized, which emphasizes the different interaction mechanism of the G4 dendrimer assemblies binding to the CD and the hydroxyundecanethiol SAMs (see above).

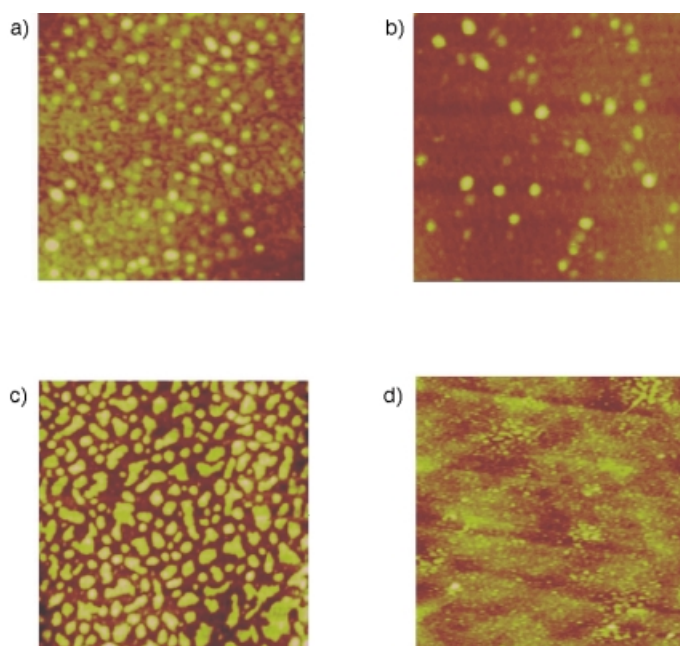


Figure 3. Tapping-mode AFM images (500 × 500 nm): after the adsorption of G4 dendrimer–cyclodextrin assemblies onto a CD SAM on gold a), and the washing of these surface assemblies with 8 mM CD b); after the adsorption of G4 dendrimer–cyclodextrin assemblies onto a hydroxyundecanethiol SAM on gold c), the washing of these surface assemblies with 8 mM CD d).

Water did not appreciably remove the adsorbed material from either SAM. However, an 8 mM CD solution did completely remove the dendrimer islands from the hydroxyundecanethiol SAM (Figure 3 d). In contrast, a considerable number of the individual dendrimers on the CD SAM remained on the surface after treatment with 8 mM CD (Figure 3 b). Nevertheless, the diminished surface concentration is obvious. It implies a relatively high desorption rate under these conditions, and thus confirms a thermodynamic, rather than kinetic, stability.

In conclusion, these experiments show that stable assemblies on surfaces can be prepared by employing multiple, intrinsically weak supramolecular interactions. Thermodynamically stable complexes can be achieved when employing two or three host–guest interactions of the strength found in the Ad–CD system. Data on the G4 dendrimer, which probably employs at least four such interactions, indicate that the kinetics can be tuned from very slow desorption in pure water to relatively fast (in the order of minutes) at high CD concentrations. The removal of material in the AFM experiment and the absence of desorption during SPR may be attributed to different thermodynamic equilibrium concentrations, or maybe to different desorption rates for individual dendrimers, compared to dendrimers packed in a full layer. More detailed kinetic experiments, possibly in flow setups, may validate the model in a more quantitative way.

This work may open new ways of preparing structured surfaces, essential for nanotechnological, electronic, or bio-chip applications. It shows that host surfaces can be employed as molecular printboards on which molecules can be placed in a firm manner, based solely on specific host–guest interactions, and addressed individually.

## Experimental Section

CD SAMs on gold were prepared by the immersion of a clean gold substrate (200 nm thick gold film on 2.54 cm glass wafers, coated with 2 nm Ti) in a solution of the CD heptathioether adsorbate (100 mg L<sup>−1</sup>) in ethanol/chloroform (2:3) for 16 h at 60 °C.

A typical SPR experiment consisted of increasing the concentration of G4–CD<sub>32</sub> in solution from 1 to 10 μM in several steps. At 10 μM, full surface coverage was reached rapidly. When a stable signal was obtained, the solution was replaced with 0.01 M HCl. This led to a decrease of the signal through both desorption of CD molecules from the surface assemblies and to a change in the bulk refractive index. No subsequent slow desorption, which might indicate desorption of the dendrimers, was observed. To probe desorption, the cell was flushed with 8 mM CD in 0.01 M HCl. As a result of a change of the bulk refractive index, the signal increased. After a stable signal was obtained, the cell was flushed with water and the signal was recorded again, which then became comparable to the signal obtained before attempted desorption.

For AFM measurements, SAMs of the CD heptathioether adsorbate and of hydroxyundecanethiol were briefly exposed (20–30 s) to a drop of a 0.5 μM solution of G4 and rinsed with water. The samples were dried under a stream of N<sub>2</sub> and imaged by using tapping-mode AFM (TM-AFM).

Received: June 28, 2002

Revised: August 22, 2002 [Z19631]

- [1] a) C. Joachim, J. K. Gimzewski, A. Aviram, *Nature* **2000**, 408, 541; b) M. A. Reed, *MRS Bull.* **2001**, 113; c) J. M. Tour, *Acc. Chem. Res.* **2000**, 33, 791; d) *Molecular Electronics: Science and Technology* (Ed.: A. Aviram), American Institute of Physics, New York, **1992**.
- [2] a) A. D. Mehta, M. Rief, J. A. Spudich, D. A. Smith, R. M. Simmons, *Science* **1999**, 283, 1689; b) S. Weiss, *Science* **1999**, 283, 1676; c) *Molecular and Biomolecular Electronics* (Ed.: R. R. Birge) American Chemical Society, Washington, **1991**.
- [3] a) A. Ulman, *An Introduction to Ultrathin Organic Films*, Academic Press, San Diego **1991**; b) H. O. Finklea in *Electroanalytical Chemistry*, Vol. 19 (Eds.: A. J. Bard, I. Rubinstein), Marcel Dekker, New York, **1996**, pp. 109–335.
- [4] a) R. D. Piner, J. Zhu, F. Xu, S. Hong, C. A. Mirkin, *Science* **1999**, 283, 661; b) S. Hong, J. Zhu, C. A. Mirkin, *Science* **1999**, 286, 523; c) L. M. Demers, C. A. Mirkin, *Angew. Chem.* **2001**, 113, 3159; *Angew. Chem. Int. Ed.* **2001**, 40, 3069; d) A. Ivanisevic, C. A. Mirkin, *J. Am. Chem. Soc.* **2001**, 123, 7887; e) K.-B. Lee, S.-J. Park, C. A. Mirkin, J. C. Smith, M. Mrksich, *Science* **2002**, 295, 1702; f) L. M. Demers, D. S. Ginger, S.-J. Park, Z. Li, S.-W. Chung, C. A. Mirkin, *Science* **2002**, 296, 1836.
- [5] a) J. J. Michels, M. W. P. L. Baars, E. W. Meijer, J. Huskens, D. N. Reinhoudt, *J. Chem. Soc. Perkin Trans. 2* **2000**, 1914; b) J. J. Michels, J. Huskens, D. N. Reinhoudt, *J. Chem. Soc. Perkin Trans. 2* **2002**, 102.
- [6] M. W. J. Beulen, J. Bügler, B. Lammerink, F. A. J. Geurts, E. M. E. F. Biemond, K. G. C. van Leerdam, F. C. J. M. van Veggel, J. F. J. Engbersen, D. N. Reinhoudt, *Langmuir* **1998**, 14, 6424.
- [7] a) H. Schönherr, M. W. J. Beulen, J. Bügler, J. Huskens, F. C. J. M. van Veggel, D. N. Reinhoudt, G. J. Vancso, *J. Am. Chem. Soc.* **2000**, 122, 4963; b) M. W. J. Beulen, J. Bügler, M. R. de Jong, B. Lammerink, J. Huskens, H. Schönherr, G. J. Vancso, B. A. Boukamp, H. Wieders, A. Offenhäuser, W. Knoll, F. C. J. M. van Veggel, D. N. Reinhoudt, *Chem. Eur. J.* **2000**, 6, 1176.
- [8] M. R. de Jong, J. Huskens, D. N. Reinhoudt, *Chem. Eur. J.* **2001**, 7, 4164.
- [9] In this model, a guest with  $n$  interaction sites for cyclodextrin is assumed to have equal intrinsic binding strengths,  $K_i$ , with CD in solution as well as at the surface. The sequential binding events occur thus with binding strength  $K_1$  to  $K_n$ , where  $K_j = (n + 1 - j) \times K_i/j$ . The free CD concentration at the surface,  $[CD]_{surf}$ , used in the equilibrium for the interaction of the first binding site to the surface, is equal to the number of moles of surface CDs divided by the sample volume. For successive surface interactions, the free CD concentration is equal to the effective molarity, estimated from molecular mechanics to be about 1 M, multiplied by the fraction of free CD surface sites ( $= [CD]_{surf}/[CD]_{surf, total}$ ). The model will be described in full detail in a future publication.



- [10] FTIR difference spectroscopy showed asymmetric and symmetric methylene stretching vibrations characteristic for the G4-CD assemblies at 2852 and 2916  $\text{cm}^{-1}$ , respectively, as well as a broad band centered around 3250  $\text{cm}^{-1}$  for the vibrations of ammonium, urea, and hydroxyl protons of the dendrimer and CD.
- [11] XPS analysis confirmed the adsorption of the G4-CD<sub>32</sub> assemblies by an increase in  $\text{N}_{1s}$  and a decrease in  $\text{S}_{2p}$  signals, which are most indicative of adsorption. Moreover, the  $\text{C}_{1s}$  and  $\text{O}_{1s}$  signals increased and decreased, respectively.
- [12] Advancing contact angles are  $68 \pm 2^\circ$  and approximately  $20^\circ$  before and after adsorption of G4 assemblies onto the CD SAMs, respectively.
- [13] EIS was performed with an external redox couple at the open cell potential. From the Nyquist plot, the charge-transfer resistance was determined by using an equivalent Randles circuit. When the negatively charged  $[\text{Fe}^{\text{III}}(\text{CN})_6]^{3-}/[\text{Fe}^{\text{II}}(\text{CN})_6]^{4-}$  couple was used, the charge-transfer resistance decreased from 38 to 3  $\text{k}\Omega$ , because the electrostatic attraction by the dendritic core facilitates the oxidation/reduction at the electrode surface.
- [14] The apparently slow adsorption as shown in the first parts of Figure 2 a upon increase of the G4 concentration can be attributed to diffusion of G4 in solution, since the adsorption in the SPR setup leads to a depletion of the liquid above the surface of  $> 100 \mu\text{m}$ , while diffusion in solution over such distances probably takes more than 1 s.

## QMOF-1 and QMOF-2: Three-Dimensional Metal–Organic Open Frameworks with a Quartzlike Topology\*\*

Jinyu Sun, Linhong Weng, Yaming Zhou, Jinxi Chen, Zhenxia Chen, Zhicheng Liu, and Dongyuan Zhao\*

The construction of metal–organic framework (MOF) coordination polymers is currently receiving considerable attention owing to their potential properties as functional solid materials, as well as their fascinating framework structures.<sup>[1–3]</sup> Particularly widely explored have been MOFs with porous chiral structures in which chiral ligands, chiral templates, or chiral functionalization of achiral zeolites are used to perform enantioselective separations and syntheses.<sup>[4–7]</sup> It is challenging to prepare chiral MOF materials with known chiral topology from an achiral building unit.

[\*] Prof. Dr. D. Zhao, Dr. L. Weng, Dr. Y. Zhou, Dr. J. Chen, Z. Chen, Z. Liu

Department of Chemistry  
Fudan University  
Shanghai, 200433 (P.R. China)  
Fax: (+86)21-6564-1740  
E-mail: dyzhao@fudan.edu.cn

J. Sun  
Department of Chemistry  
Liaoning University, Shenyang,  
110036 (P.R. China)

[\*\*] This work was supported by the NSF of China (Grants No. 29925309), the Chinese Ministry of Education, the Shanghai Science Foundation (C00JC14014) and the State Key Basic Research Program of PRC (G200048001). We thank Dr. Y. Yan, Dr. L. Huang, and Dr. H. Wang of U.C.-Riverside for helpful discussions.



Supporting information for this article is available on the WWW under <http://www.angewandte.org> or from the author.

Learning from nature's minerals, and utilizing the well-defined coordination geometries of metal centers, some structures of minerals with specific functionality, such as perovskite,<sup>[8]</sup> rutile,<sup>[9]</sup> PtS,<sup>[10]</sup> and feldspar<sup>[11]</sup> have been artificially produced by replacing monoatomic anions ( $\text{O}^{2-}$ ,  $\text{S}^{2-}$ ) with polyatomic organic  $\mu$  ligands. The quartz phase, which is chiral, has unique piezoelectricity and thermally sensitive properties and is widely used in resonators and sensors.<sup>[12]</sup> Although the  $\text{SiO}_2$  phase with quartz topology is thermodynamically more stable than cristobalite which has diamond topology, in nature or in artificial materials, known phases which have quartz topology are rare with only one example, a cyano-bridged coordination polymer, reported by Robson and co-workers.<sup>[13]</sup> Generally, most materials comprising four-connected tetrahedral (T) units, including MOFs, exist in the diamond topology,<sup>[1c,d,14]</sup> rather than the quartz topology, while  $\text{SiO}_2$  and  $\text{GeO}_2$  are minerals that have both a quartz polymorph and cristobalite with diamond topology. Interestingly, when cristobalite is quenched to room temperature,<sup>[15]</sup> it is transformed reconstructively to the quartz polymorph.

Herein we report the preparation of two quartzlike, chiral, open MOFs,  $\text{Zn}(\text{ISN})_2 \cdot 2\text{H}_2\text{O}$  (ISN = isonicotinate), assigned QMOF-1, with the low symmetry of  $\alpha$ -quartz and  $\text{InH}(\text{BDC})_2$  (BDC = terephthalate), QMOF-2, with the high symmetry of  $\beta$ -quartz. QMOF-1 with a large ( $\sim 8.6 \text{ \AA}$ ) left-handed channel was successfully synthesized with an asymmetric ISN ligand by using a low-temperature diffusion method (room temperature) similar to the preparation of metal carboxylate<sup>[17]</sup>. On using a highly distorted complex anion  $[\text{In}(\text{O}_2\text{CR})_4]^-$  as the T block,<sup>[16]</sup> and terephthalate as a linear rod, we could assemble the anion-type  $\beta$ -quartzlike network QMOF-2 with a right-handed channel ( $\sim 7.8 \text{ \AA}$ ).

The preparation of QMOF-1 was carried out in a wide range of conditions:  $\text{Zn}(\text{NO}_3)_2 \cdot 6\text{H}_2\text{O}$ : 1.5–3.0 ISN: 1–10 triethylamine (TEA): 5–10000 dimethylsulfoxide (DMSO): 0–20000 ethanol. After one week, large colorless needlelike single crystals with dimensions up to  $0.200 \times 0.200 \times 3 \text{ mm}$  were obtained quantitatively (relative to Zn). QMOF-2 was solvothermally obtained from  $\text{InCl}_3$ :terephthalate (1:2) at  $160^\circ\text{C}$  for 3 days, yield 60 % (relative to In). The IR spectra showed that the carboxylate group in QMOF-1 has monodentate coordination to the metal center, while that in QMOF-2 is bidentate.<sup>[18]</sup>

The single-crystal X-ray diffraction studies reveal that all the zinc ions in QMOF-1 are four-coordinate (Figure 1a).<sup>[19]</sup> Each Zn atom is coordinated by two nitrogen atoms of two ISN ligands and two oxygen atoms of two carboxylate groups from two other ISN ligands. All of the T units are slightly distorted, the Zn–O and Zn–N bonds are 1.95 and 2.02  $\text{\AA}$ , respectively, and the angles of N(1)–Zn(1)–N(2), N(1)–Zn(1)–O(2), N(1)–Zn(1)–O(1), O(1)–Zn(1)–O(2) are 113.5, 117.5, 104.9, 100.4°, respectively. The 3D twofold interpenetrated network with T blocks is characteristic of a  $6^48^2$ -b net, similar to that of  $\alpha$ -quartz (Figure 2, Figure S1 in the supporting information).<sup>[1c]</sup> In the QMOF-1 structure, large Zn cations replace the Si atoms in quartz structure, and the long ISN anions replace the O atoms, so that the separation between two T units can be expanded to 8.813  $\text{\AA}$ , only slightly different from the Zn–Zn separations in the diamondoid network